

# A LOW-COST AND ROBUST MULTIMODAL WIRELESS NETWORK WITH ADAPTIVE ESTIMATOR AND GLRT DETECTOR

Jianjun Chen<sup>1</sup>, John Aa. Sørensen<sup>2</sup>, Zoltan Safar<sup>3</sup> and Kåre J. Kristoffersen<sup>1</sup>

<sup>1</sup>Department of Innovation, IT University of Copenhagen, Rued Langgaards Vej 7, 2300 Copenhagen S., Denmark  
email: {chen, kjk}@itu.dk

<sup>2</sup>Department of Electrical Engineering and Information Technology, Copenhagen University College of Engineering  
Lautrupvang 15, 2750 Ballerup, Denmark. email: jaas@ihk.dk

<sup>3</sup>Modem System Design, Nokia, Copenhagen, Denmark. email: zoltan.2.safar@nokia.com

## ABSTRACT

The problem of using a multiple-node indoor wireless network as a distributed sensor network for detecting physical intrusion is addressed. The challenges for achieving high system performance are analyzed. A high-precision adaptive estimator and a high-precision signal level change estimator are derived. Based on the low computational complexity of the estimators, a low-cost and robust system architecture is proposed. Experiments show that the proposed system performs significantly better than the published prototype multimodal wireless network system.

## 1. INTRODUCTION

In WLAN environments, moving objects/humans can cause significant variations in the received signal strength and the RMS delay spread. This has been shown in previous experiments [1]. By detecting this kind of variations in an indoor WLAN environment, we can detect physical intruders when the environment is supposed to have no human activities.

A prototype multimodal wireless network was proposed in [2]. It has multiple nodes, which are access points or stations at fixed positions. It has two modes of operation: the communication mode and the surveillance mode. In the communication mode, the network functions as a traditional WLAN. In the surveillance mode, the network functions as a distributed sensor network for detecting physical intrusion into the indoor environment in the following way: the nodes transmit one by one in a round robin fashion while the rest of the nodes receive the transmitted signal, and the received signal at each node is processed to extract some relevant characteristics of the propagation environment. Then, the obtained information at the nodes is combined and processed by the fusion center to decide whether there is an physical intruder in the environment or not.

The prototype multimodal network was shown to have promising intrusion detection capabilities [2]. However, given the model of the received signal, the challenges for achieving high system performance has not been analyzed. Moreover, the problem of adaptive parameter estimation has not been addressed, which is important in order to avoid system performance degradation caused by slow signal drift. In this paper, we analyze the challenges for such a system to achieve high performance. A high-precision adaptive estimator with Kalman filter is derived in Section 4, and a high-precision signal level change estimator is derived in Section 5. Based on the derivation, we propose a low-cost and robust system architecture in Section 6. We demonstrate the performance of our system by simulations and experiments.

## 2. BACKGROUND

Here we first describe the signal model used in both [2] and this paper. Consider such a network consisting of  $N$  nodes. The model of received signal parameters of interest, for example the received signal strength at the receiver node  $n$  from the transmitter node  $m$  ( $m \neq n$ ) at some discrete time  $t$  is shown in Figure 1. The true

value of the received signal parameter (the signal strength information in dBm is used in our experiments),  $l_{m,n}^0(t)$ , is biased by an unknown  $B_{m,n}$ , resulting in the biased parameter,  $l_{m,n}(t)$ , which is assumed to be between  $l_{MIN}$  and  $l_{MAX}$ . The bias  $B_{m,n}$  comes from some measurement inaccuracy due to non-calibrated or non-standardized transmitted and received signal properties, such as the determination of the IEEE 802.11 transmit power and Received Signal Strength Index (RSSI) value. Due to the bias, in general,  $l_{m,n}(t) \neq l_{n,m}(t)$ , even if the channel is reciprocal. The  $l_{m,n}(t)$  is further disturbed by a zero-mean, white Gaussian noise  $z_{m,n}(t)$  with variance  $\sigma_n^2(t)$ , resulting in a noisy and biased signal parameter value  $x_{m,n}(t)$ . Then,  $x_{m,n}(t)$  is passed through a quantizer to produce a quantizer index,  $y_{m,n}(t)$ , as the observation. The quantizer is assumed to have  $2^b$  levels. We denote the decision regions by  $a(0) < a(1) < \dots < a(2^b)$ , in which  $a(0) = l_{MIN}$  and  $a(2^b) = l_{MAX}$ , and the quantizer maps the input value  $x$  to the quantizer index  $y \in \{0, 1, \dots, 2^b - 1\}$  if  $a(y) < x \leq a(y+1)$ .

In [2], the proposed detection procedure consists of a training phase and a detection phase. If there is no intrusion, the signal parameters are assumed to be constant, such that  $l_{m,n}(t) = l_{m,n}$  and  $\sigma_n(t) = \sigma_n$ . During the training phase,  $l_{m,n}$  and  $\sigma_n$  are estimated by using a large number ( $T = 10^3$ ) of observations. In the detection phase, the system carries out a cyclic scanning of the environment. At the end of each cycle, the parameters  $l_{m,n}$  are re-estimated based on a small number ( $T = N_c = 50$ ), where  $N_c$  is the number of observations during one scanning cycle for each pair of transmitter and receiver nodes) of observations. This leads to the estimate of the change  $\Delta l_{m,n}$  of each  $l_{m,n}$ . The parameters  $\sigma_n$  are assumed to be unchanged, since even if there is an intruder, he will not impact the noise parameters  $\sigma_n$ . At the end of each cycle, the system decides whether there is an intruder in the indoor environment or not. This is done by detecting whether there are significant changes  $\Delta l_{m,n}$  in the parameters  $l_{m,n}$  (Hypothesis  $\mathcal{H}_1$ ) or not (Hypothesis  $\mathcal{H}_0$ ). In this way, the problem is formed as a composite hypothesis testing problem [3].

In the training phase, for each node  $n$ , from its observations of the other nodes, we need to estimate the parameters  $\sigma_n$  and  $\mathbf{l}_n = [l_{1,n}, \dots, l_{n-1,n}, l_{n+1,n}, \dots, l_{N,n}]^T$  related to it. Given the observations  $\mathbf{y}$  (which contains  $T$  observations of every other node), the log-likelihood function of the parameters is given by [2]:

$$\ln P(\mathbf{y} = \mathbf{i}; \mathbf{l}_n, \sigma_n) = \sum_{m=1}^N \sum_{t=1}^T \ln F(l_{m,n}, \sigma_n, i_{m,n}(t)) \quad (1)$$

where the vector  $\mathbf{i} = \{i_{m,n}(t) | 1 \leq t \leq T, 1 \leq m \leq N, m \neq n\}$  is an observed realization of  $\mathbf{y}$ , and

$$F(l, \sigma, j) = \frac{1}{\sqrt{2\pi}\sigma} \int_{a(j)}^{a(j+1)} e^{-\frac{(v-l)^2}{2\sigma^2}} dv. \quad (2)$$

In [2], the maximum likelihood (ML) estimates of  $l_{m,n}$  and  $\sigma_n$ ,  $\hat{l}_{m,n}$  and  $\hat{\sigma}_n$ , were obtained by letting  $\frac{\partial \ln P(\mathbf{y} = \mathbf{i}; \mathbf{l}_n, \sigma_n)}{\partial l_{m,n}} = 0$  ( $1 \leq m \leq N, m \neq n$ )

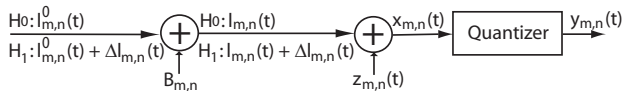


Figure 1: The received signal model

and  $\frac{\partial \ln P(\mathbf{y}=\mathbf{i}; \mathbf{l}_n, \sigma_n)}{\partial \sigma_n} = 0$ , and solving these equations. Two estimators were derived in [2] to solve these equations. An iterative ML estimator was obtained by solving them with Newton's method. An approximate ML estimator was obtained by direct calculation, when regarding the effect of the quantizer as the additive white noise.

In the detection phase, as mentioned earlier and as shown in Fig.1, the signal parameter changes  $\hat{\Delta} l_{m,n}$  were estimated by re-estimating  $l_{m,n}$  at the end of each scanning cycle. A generalized likelihood ratio test (GLRT) detector was given in [2] to solve this composite hypothesis testing problem. Let  $\gamma$  denote the decision threshold, then the system decides  $\mathcal{H}_1$  if

$$\sum_{n=1}^N g_n > \ln \gamma \quad (3)$$

where  $g_n$  is given by

$$g_n = \sum_{m=1}^N \sum_{t=1}^T \ln \frac{F(\hat{l}_{m,n} + \hat{\Delta} l_{m,n}, \hat{\sigma}_n, i_{m,n}(t))}{F(\hat{l}_{m,n}, \hat{\sigma}_n, i_{m,n}(t))}. \quad (4)$$

### 3. PROBLEM ANALYSIS

The prototype multimodal wireless network presented in [2] was shown by experiments to have promising capabilities of physical intrusion detection. To make such a system become high-performance and robust, more research is needed. The challenges for achieving high performance of intrusion detection are analyzed in Section 3.1. The problem of adaptive parameter estimation is described in Section 3.2. Our solutions to these problems are given in the following sections.

#### 3.1 Challenges for Achieving Optimal System Performance

In [2], the composite hypothesis testing problem is solved by the GLRT detector (3). The performance of the GLRT detector relies on the precision of the ML estimates of the signal parameters  $l_{m,n}$ ,  $\sigma_n$  and  $\Delta l_{m,n}$  [3]. Therefore, in order to achieve the optimal detection performance in the GLRT detector, it is necessary to find good estimators for the parameters  $l_{m,n}$ ,  $\sigma_n$  and  $\Delta l_{m,n}$ .

The task of estimating the signal parameters  $l_{m,n}$ ,  $\sigma_n$  and  $\Delta l_{m,n}$  is not trivial, because the observations  $i_{m,n}(t)$  are very rough quantization of the received signal. Here we illustrate this problem by experimental data. We let a multimodal wireless network with 3 nodes scan the environment cycle by cycle as described in Section 2. The experiment was done at a corner of the IT University of Copenhagen for around 100 minutes, when there was no human activities at the experimental site. We divide the observations into windows and let each window contain  $T = 10^3$  observations (each window contains 20 cycles, and each path has  $N_c = 50$  observations in every cycle). Then we use the iterative ML estimator given in [2] to estimate the signal parameters  $l_{1,2}$ ,  $l_{3,2}$  and  $\sigma_2$  from the observations  $i_{1,2}(t)$  and  $i_{3,2}(t)$  ( $1 \leq t \leq T$ ) in each of the windows. One RSSI observation sequence (transmitted by node 3 and observed by node 2) is shown in Figure 2(A), the window-wise estimates  $\hat{l}_{3,2}$  are shown in 2(B), and the window-wise estimates  $\hat{\sigma}_2$  are shown in Figure 2(C). As we can see, there are only three different RSSI values (quantizer indices) observed during the time, which is because the received signal is very roughly quantized, since the  $\sigma_n$  is much smaller than the quantization step size  $q$ . In these experimental data, the estimates of  $\sigma_2$  were in the range  $(0.3q, 0.4q)$ , where  $q = 1$ .

Usually when the quantization errors are regarded as white noise and uniformly distributed in  $(-q/2, q/2)$ , the well-known Sheppard's corrections can be used to estimate the mean and variance of the signal before quantization [4]. If the input signal to the quantizer is Gaussian distributed  $N(\mu, \sigma^2)$ , this noise model of the quantization error is suitable if  $\sigma \geq 0.7q$ , but it is not suitable if

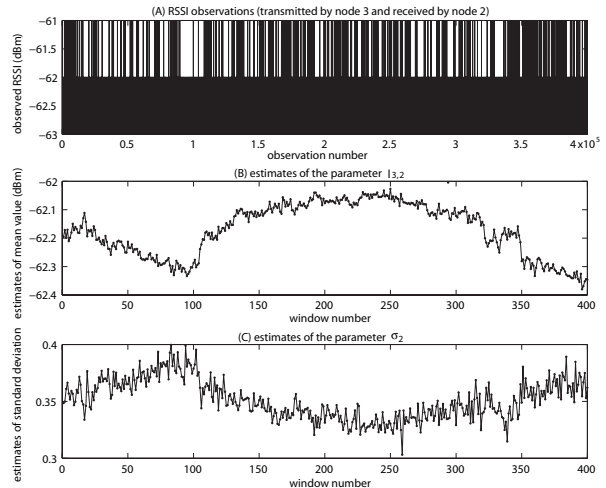


Figure 2: RSSI observations and window-wise iterative ML estimates of the signal parameters

$\sigma < 0.7q$ , otherwise the biases of the estimates  $\hat{\mu}$  and  $\hat{\sigma}$  are large [4]. When the quantizer in Fig.1 is uniform with quantization step size  $q$ , the approximate ML estimator proposed in [2] for estimating  $l_{m,n}$  becomes the formula of the Sheppard's corrections for estimating the mean value. Therefore, the approximate ML estimator will not perform well in our application due to the rough quantization.

It becomes more difficult to analyze the performance of the iterative ML estimator in [2], which is due to the non-linear characteristic of the ML estimator and the effect of the quantizer. Figure 2 shows that the iterative ML estimator works well even when  $\sigma_n$  is as small as around  $0.35q$ .

We can see that in (1), many components of the observation vector  $\mathbf{i} = \{i_{m,n}(t)\}$  are identical because of the rough quantization. Assume that in the  $T$  observations of the node pair from  $m$  to  $n$ , there are  $T_{m,n}$  different values,  $i'_{m,n}(k)$ , ( $1 \leq k \leq T_{m,n}$ ), and each item  $i'_{m,n}(k)$  appears  $N_{m,n}(k)$  times specifically, such that  $\sum_{k=1}^{T_{m,n}} N_{m,n}(k) = T$ . Then the log-likelihood function (1) can be written as

$$\ln P(\mathbf{y}=\mathbf{i}; \mathbf{l}_n, \sigma_n) = \sum_{m=1}^N \sum_{k=1}^{T_{m,n}} N_{m,n}(k) \ln F(l_{m,n}, \sigma_n, i'_{m,n}(k)). \quad (5)$$

Equation (5) shows that the ML estimates of the parameters  $l_{m,n}$  and  $\sigma_n$  rely on the values of  $T_{m,n}$  and  $N_{m,n}(k)$ , where  $1 \leq k \leq T_{m,n}$ .

The iterative ML estimator will encounter a "lack of information" problem originating from very rough quantization. In order to simplify the discussion, we first consider a network containing only 2 nodes, namely  $N = 2$ . Then, the ML estimates of  $l_{2,1}$  and  $\sigma_1$  need to be estimated from  $i_{2,1}(t)$ , ( $1 \leq t \leq T$ ). In the extreme case of the "lack of information" when all the observations are identical, namely  $i_{2,1}(t)$  equals to some quantizer index  $j$  for all  $1 \leq t \leq T$ , obviously the iterative ML estimator will generate the estimates  $\hat{\sigma}_1 \rightarrow 0$  and  $\hat{l}_{2,1}$  can be any value in the range  $(a(j), a(j+1))$ . We will not consider this extreme case in this paper, because its probability is ignorable when  $T$  is not too small.

The other case of the "lack of information" phenomenon is when only two neighbouring quantization indices  $j$  and  $j+1$  appear in the observations  $i_{2,1}(t)$ , ( $1 \leq t \leq T$ ), as shown in Figure 3. When this happens, (5) becomes

$$\ln P(\mathbf{y}=\mathbf{i}; \mathbf{l}_n, \sigma_n) = N_{2,1}(1) \ln F(l_{2,1}, \sigma_1, j) + N_{2,1}(2) \ln F(l_{2,1}, \sigma_1, j+1) \\ = N_{2,1}(1) \ln F(l_{2,1}, \sigma_1, j) + (T - N_{2,1}(1)) \ln F(l_{2,1}, \sigma_1, j+1). \quad (6)$$

By regarding  $F(l_{2,1}, \sigma_1, j)$  and  $F(l_{2,1}, \sigma_1, j+1)$  as variables, the maximization of the log-likelihood function in Equation (5) is the maximization of (6) with the following constraints:

$$\begin{aligned} 0 &\leq F(l_{2,1}, \sigma_1, j) \leq 1 \\ 0 &\leq F(l_{2,1}, \sigma_1, j+1) \leq 1 \\ 0 &\leq F(l_{2,1}, \sigma_1, j) + F(l_{2,1}, \sigma_1, j+1) \leq 1 \end{aligned}$$

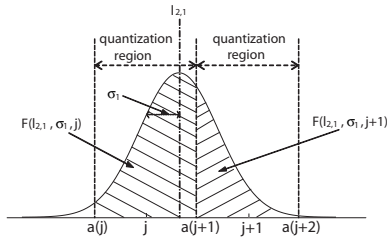


Figure 3: Quantization indices and decision regions, and a Gaussian distributed signal

The solution to this fundamental optimization problems is,

$$\begin{aligned} F(l_{2,1}, \sigma_1, j) &= N_{2,1}(1)/T \\ F(l_{2,1}, \sigma_1, j+1) &= 1 - N_{2,1}(1)/T. \end{aligned}$$

However, as shown in Figure 3, this is satisfied only if  $\hat{\sigma}_1 \rightarrow 0$  and  $\hat{l}_{2,1} \rightarrow a(j+1)$ , which is the decision boundary between the indices  $j$  and  $j+1$ . Unfortunately, this solution is not reasonable, because  $\sigma_1$  is the standard deviation of the thermal noise and should never be zero.

Now consider the general case when a network contains more than 2 nodes. At the node  $n$ , the ‘‘lack of information’’ phenomenon happens when there are only two neighbouring quantizer indices appearing in every observations path  $l_{m,n}(t)$ , ( $1 \leq t \leq T$ ), then the ML estimator will generate  $\hat{\sigma}_n \rightarrow 0$ . This can be derived very similarly to the steps above. The reason for this phenomenon is that we do not have enough information to infer the parameter  $\sigma_n$ , which originates from the rough quantization. The probability of this phenomenon is small when  $T$  is large as in the training phase ( $T = 10^3$ ) [2]. However, this probability is not small when  $T$  is small as in the detection phase ( $T = N_c = 50$ ). For example, as shown in Figure 3, if  $F(l, \sigma, j) + F(l, \sigma, j+1) = 0.995$ , then the probability of this phenomenon is  $0.995^T$ , and it is around 0.007 when  $T = 10^3$ , however it is around 0.778 when  $T = 50$ .

This ‘‘lack of information’’ phenomenon does not originate in the iterative ML estimator, it is the problem of not having enough information to estimate the parameters, which is caused by the rough quantization. Since the performance of the GLRT detector relies on parameter estimation precision, to achieve optimal performance in the GLRT detector, this problem must be solved satisfyingly. In other words, when the ‘‘lack of information’’ phenomenon happens, a good estimator should still be able to get good estimates of the parameters. Our solution to this is given in Section 4 and 5.

### 3.2 Need for Adaptive Estimation of The Parameters

Over a long time period, the signal parameters  $l_{m,n}(t)$  and  $\sigma_n(t)$  tend to drift slowly to significantly different levels due to changes in the environment or in the sensor node hardware. A clear example of the observed slowly drifting RSSI is shown in Figure 2.

Since the performance of the GLRT detector relies on the estimation precision of the parameters, it is necessary to adapt the estimates to the moderately drifting signal parameters to avoid system performance degradation. Switching between the training and detection phases to handle the drift is not a good solution, because the detection functionality is off during the training phase.

In order to achieve a good intrusion detection performance and avoid false alarm, we derive an adaptive estimator with Kalman filter in Section 4 to solve this problem.

## 4. ADAPTIVE ESTIMATOR WITH KALMAN FILTER

We let the detection procedure consist of the training and detection phases as proposed in [2]. The detection carries out a cyclic scanning of the environment. However, in the detection phase, as long as the hypothesis  $\mathcal{H}_1$  has not been decided yet, the observations in the past scanning cycles are used to adapt the estimates of the parameters. This differs from the prototype system in [2].

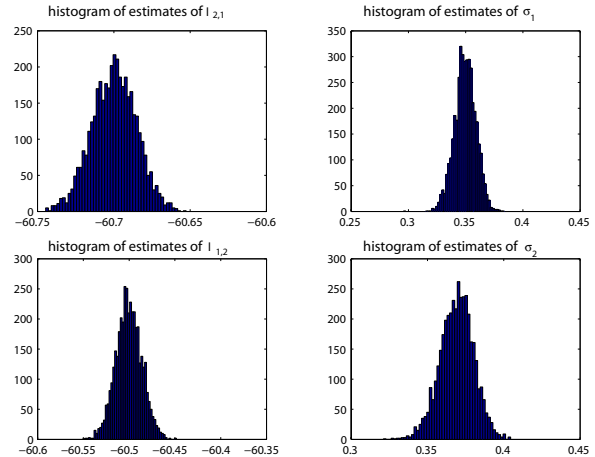


Figure 4: histogram of the estimates of the parameters

Since the hypothesis decision is made only at the end of every cycle, we only need to adapt the estimates of the parameters at most once every cycle. To reduce the computational load, we choose to adapt the estimates once every multiple (say,  $N_s$ ) cycles. This is suitable due to the slow drift of the signal parameters, because a sudden change is regarded as the happening of physical intrusion.

Note that if we combine the observations of every  $N_s$  cycles to form an observation window with size  $T = N_s \times N_c$ , we can use the iterative ML estimator in [2] to estimate the parameters within the window. In this way, when the system runs, we can get a sequence of estimates for each parameter. Such estimation sequences are shown in Figure 2(B) and 2(C). By appropriate modelling the estimation sequences, we propose an adaptive estimator in this section.

Here we briefly demonstrate that the computational complexity of the iterative ML estimator can be highly reduced. In (5), by letting the partial derivatives of the log-likelihood function equal to zero, namely  $\frac{\partial \ln P(\mathbf{y}=\mathbf{i}; l_n, \sigma_n)}{\partial l_{m,n}} = 0$  ( $1 \leq m \leq N, m \neq n$ ) and  $\frac{\partial \ln P(\mathbf{y}=\mathbf{i}; l_n, \sigma_n)}{\partial \sigma_n} = 0$ , we get  $N$  equations

$$f_1(l_{m,n}, \sigma_n) = \sum_{k=1}^{T_{m,n}} N_{m,n}(k) \frac{X(l_{m,n}, \sigma_n, i'_{m,n}(k)) - X(l_{m,n}, \sigma_n, i'_{m,n}(k) + 1)}{F(l_{m,n}, \sigma_n, i'_{m,n}(k))} = 0 \quad (7)$$

$$f_2(l_n, \sigma_n) = \sum_{m=1}^N \sum_{k=1}^{T_{m,n}} N_{m,n}(k) \psi(l_{m,n}, \sigma_n, i'_{m,n}(k)) = 0, \quad (8)$$

where  $X(l, \sigma, j) = e^{-\frac{(a(j)-l)^2}{2\sigma^2}}$ , and

$$\psi(l, \sigma, j) = \frac{(a(j) - l)X(l, \sigma, j) - (a(j+1) - l)X(l, \sigma, j+1)}{F(l, \sigma, j)}.$$

Equations (7) and (8) can be solved by Newton’s method, which is shown in [2]. However, the computational complexity is no more linear with the window size  $T$ , but becomes constant ( $T_{m,n}$  can be regarded as a small constant around 3 as shown in Figure 2(A)).

Due to the non-linearity of the ML estimator and the effect of the quantizer, it is not possible to give the distribution of  $\hat{l}_{m,n}$  and  $\hat{\sigma}_n$  in closed form. However, when the likelihood function satisfies the regularity conditions, the ML estimates of the parameters are asymptotically Gaussian around the true parameter values [6]. Therefore, here the  $\hat{l}_{m,n}$  and  $\hat{\sigma}_n$  can be approximated as Gaussian distributed when  $T$  is large. We illustrate this by an example. We simulate a 2-node system with parameters  $l_{1,2} = -60.5$ ,  $l_{2,1} = -60.7$ ,  $\sigma_1 = 0.35$ ,  $\sigma_2 = 0.37$  and  $T = 10^3$ . The histogram of  $\hat{l}_{1,2}$ ,  $\hat{l}_{2,1}$ ,  $\hat{\sigma}_1$ ,  $\hat{\sigma}_2$  are shown in Figure 4. As we can see, these estimates are approximately Gaussian distributed.

From the above discussion, it is clear that in each observation window, the estimation errors  $\hat{l}_{m,n} - l_{m,n}$  and  $\hat{\sigma}_n - \sigma_n$  can be regarded as zero-mean Gaussian noise (for convenience, here we let  $l_{m,n}$  and

$\sigma_n$  denote the true values within the window). When the signal parameters drift slowly, the estimation sequence of each parameter can be regarded as a slowly drifting signal disturbed by an AWGN. Therefore, the Kalman filter is the optimal solution to filter these estimation sequences for improving the estimation precision. By regarding these random variable  $\hat{l}_{m,n}$  and  $\hat{\sigma}_n$  as independent of each other, we get the following simple state-space model:

$$\mathbf{x}(k) = \mathbf{x}(k-1) + \mathbf{u}(k) \quad (9)$$

$$\mathbf{y}(k) = \mathbf{x}(k) + \mathbf{v}(k) \quad (10)$$

where  $\mathbf{x}(k)=[\hat{l}_{1,n}, \dots, \hat{l}_{n-1,n}, \hat{l}_{n+1,n}, \dots, \hat{l}_{N,n}, \hat{\sigma}_n]^T$  is the signal vector,  $\mathbf{y}(k)$  is the observation vector. The excitation noise vector  $\mathbf{u}(k)$  and the observation noise vector  $\mathbf{v}(k)$  are both zero-mean AWGN.

The variance of each coordinate of  $\mathbf{u}(k)$  and  $\mathbf{v}(k)$  are appropriately chosen with respect to the window size  $T$ , the latest adapted  $\hat{\sigma}_n$ , and the effect of the quantizer. For  $T$  observations of a random variable following the distribution  $N(l, \sigma^2)$ , the Cramer-Rao Lower Bound (CRLB) for  $l$  is  $\sigma^2/T$ , and the CRLB for  $\sigma$  is  $\sigma^2/2T$  [5]. For estimator (7), (8), the data are quantized Gaussian. Therefore, taking the quantization effect into consideration, we take the double of these CRLBs as the variances of the corresponding observation noise  $\mathbf{v}(k)$ . Namely, we let the variance of each coordinate of  $\mathbf{v}(k)$  corresponding to  $\hat{l}_{m,n}$  be equal to  $2\hat{\sigma}_n^2/T$ , and we let the variance of the last dimension of  $\mathbf{v}(k)$  be equal to  $\hat{\sigma}_n^2/T$ .

Finally, we need to handle the ‘‘lack of information’’ phenomenon. Even if  $T$  is set sufficiently large by choosing a large  $N_s$ , the phenomenon may still happen with a small probability. In this case, we will have trouble to use (7) and (8) for estimation. But we can solve this problem satisfyingly as follows. Since we have got a high-precision estimate of  $\sigma_n$  by the above adaptive estimator with Kalman filter, if the ‘‘lack of information’’ phenomenon happens in the current observation window, we can let  $\sigma_n$  be equal to the last adapted estimate, and we only need to estimate the  $l_{m,n}$  within the current observation window. In this instance, (7) becomes

$$f_1(l_{m,n}) = \sum_{k=1}^{T_{m,n}} N_{m,n}(k) \frac{X(l_{m,n}, \sigma_n, i'_{m,n}(k)) - X(l_{m,n}, \sigma_n, i'_{m,n}(k)+1)}{F(l_{m,n}, \sigma_n, i'_{m,n}(k))} = 0. \quad (11)$$

The unknown  $l_{m,n}$  in (11) can be solved by Newton’s method. In this way, the estimation sequence of each parameter can continue, and the adaptive estimator can work continuously.

Note that if the intruder want to move slowly to avoid detection by letting the adaptive estimator adapt to the changes caused by him, he must be very slow, for example less than 1cm/s.

## 5. SIGNAL LEVEL CHANGE ESTIMATOR AND GLRT DETECTOR

At the end of each scanning cycle, the signal level changes  $\Delta l_{m,n}$  need to be estimated for hypothesis testing. However, in Section 3, we have analyzed that both the approximate ML estimator and the iterative ML estimator proposed in [2] are not suitable for this task. The approximate ML estimator is biased, and the iterative ML estimator cannot handle the ‘‘lack of information’’ phenomenon due to the small  $T$ . However, this phenomenon happens with a high probability because  $T$  is a small number during each scanning cycle.

The main drawback of the iterative ML estimator is that it tries to estimate both the  $l_{m,n}$  and  $\sigma_n$  from a small number of observations ( $T = N_c$ ). However, our basic assumption is that the intruder will only cause variations in the signal parameters  $l_{m,n}$ , but not in the noise parameter  $\sigma_n$ . It is not necessary to estimate them both in every scanning cycle, because a high-precision estimate of  $\sigma_n$  has already been obtained by the adaptive estimator. Instead, at the end of each scanning cycle, to estimate the possible changes  $\Delta l_{m,n}$ , we only need to estimate the parameters  $l_{m,n}$  given the observations of that cycle. We use (11) to estimate  $l_{m,n}$  within the current scanning cycle, in which we let  $\sigma_n$  be equal to the latest adapted estimate

obtained from the adaptive estimator. The difference between the solution  $l_{m,n}$  obtained from (11) and the latest  $l_{m,n}$  obtained from the adaptive estimator is the estimate of  $\Delta l_{m,n}$  within the cycle.

The signal level change estimator proposed here has the following advantages. First, it is unbiased and has a good performance, since  $\sigma_n$  is already known with high precision. Second, even in the ‘‘lack of information’’ case with only two different quantization indices appearing, it can still produce a correct ML estimate of  $l_{m,n}$ , which is also because that  $\sigma_n$  is already known with high precision.

We resort to the GLRT detector (3) to solve this composite hypothesis testing problem. Because all the parameters,  $l_{m,n}$ ,  $\Delta l_{m,n}$  and  $\sigma_n$ , are estimated with high precision, the performance of the GLRT detector is guaranteed.

## 6. LOW-COST AND ROBUST SYSTEM ARCHITECTURE

The prototype multimodal wireless network proposed in [2] needs a powerful computer to work as the fusion center, whose task is to estimate the signal parameters in the training phase, and to estimate changes of the signal parameters at the end of each scanning cycle in the detection phase, and then use the GLRT detector for composite hypothesis testing. However, this solution is not very cost-effective due to the cost of the fusion center. Moreover, it is not very robust, since when this system is deployed in private homes, the fusion center is usually a personal computer which is under the threat of virus, network attacks, system failure, etc. These constraints limit the deployment of such kind of multimodal wireless network.

The computational task of the parameter estimation and change detection can be done in a highly distributed manner. In Section 4, an adaptive signal parameter estimator is derived. Through the derivation, it is clear that for the node  $n$ , by using this estimator and only based on its own observations, node  $n$  can estimate all the signal parameters  $\{l_{m,n}\}$  and  $\sigma_n$  related to it. Moreover, by using the signal level change estimator derived in Section 5, node  $n$  can estimate all the signal level changes  $\{\Delta l_{m,n}\}$  in every scanning cycle from its own observations, and then calculate  $g_n$ .

We propose to let the nodes of the network elect one node out of them as the fusion center. At the end of each scanning cycle, the elected fusion center sums up the logarithm of the local likelihood ratios reported from all nodes, and then compare the summation with  $\ln \gamma$  for the composite hypothesis testing. Note that the detector is centralized even though the estimator is decentralized.

Such a system architecture is low-cost, since it eliminates the need of a powerful computer as the dedicated fusion center. Moreover, it is robust, since whenever there is a failure at the current fusion center, a new node can be elected as the fusion center and the system can work with reduced number of nodes. Of course, the decision threshold  $\gamma$  needs to be adjusted in this instance. This system architecture requires that the sensor nodes are capable of the computational task, which can be easily satisfied, because the ML estimator of (7) and (8) has very low computational complexity and the Kalman filter has a very simple structure.

## 7. EXPERIMENTAL RESULTS

The performance of the derived adaptive ML estimator with Kalman filter is illustrated by simulations. In order to illustrate the drift of signal parameters, we use a slope factor  $\rho_{m,n}$ , which defines the speed of change in  $l_{m,n}(t)$ . A uniform quantizer with step size  $q = 1$  is used. We simulate a 3-node system that start with parameters:  $l_{1,2} = -60.5$  dBm,  $l_{2,1} = -60.7$  dBm,  $l_{1,3} = -53.3$  dBm,  $l_{3,1} = -53.4$  dBm,  $l_{2,3} = -70.1$  dBm,  $l_{3,2} = -70.2$  dBm,  $\sigma_1 = 0.35$ ,  $\sigma_2 = 0.37$ ,  $\sigma_3 = 0.39$ ,  $\rho_{1,2} = \rho_{2,1} = 0.0$ ,  $\rho_{1,3} = \rho_{3,1} = 0.4 \times 10^{-6}$ ,  $\rho_{2,3} = \rho_{3,2} = -0.8 \times 10^{-6}$ . The results are shown in Figure 5, in which the average mean squared error (MSE) for the signal parameters  $\{l_{m,n}\}$  and the noise parameters  $\{\sigma_n\}$  are depicted as a function of the window size  $T$ . We can see that for the estimation of the noise parameters, the adaptive ML estimator with Kalman filter performs around one order of magnitude better than the iterative ML estimator given in [2], no matter the window size  $T$  since the noise parameter is

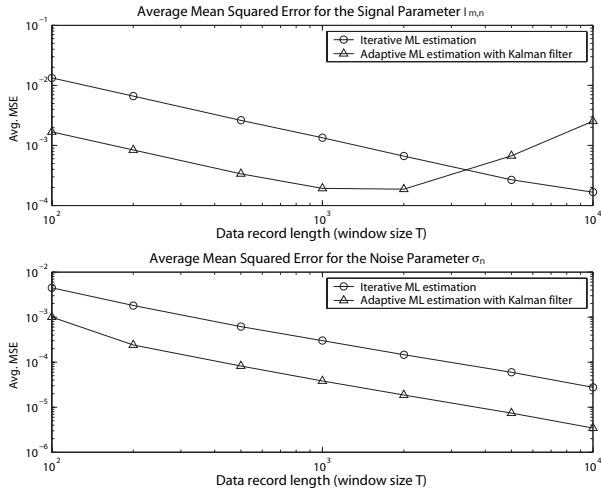


Figure 5: The simulation results

not drifting in the simulation. For the estimation of the signal parameters  $l_{m,n}$ , the larger  $T$ , the better performance the iterative ML estimator will have. When  $T$  is not too large, the adaptive estimator with Kalman filter performs around one order of magnitude better than the iterative ML estimator. However, due to the parameter drift introduced in the simulation, when  $T$  is too large ( $T = 10^4$ ), the delay effect of large window is not ignorable (the signal dynamics within the window is no more suitable to be approximated as constant, since the amount of changes within the window,  $\rho_{m,n} \times T$ , becomes significant). In this case, the adaptive estimator with Kalman filter performs even worse due to the delay effect of the Kalman filter.

We can also see from Figure 5 that the window size  $T = 10^3$  (which lasts for around 10 seconds) is appropriate in this simulation, since significant improvements are achieved with respect to the estimation performance, and the delay effect is not significant.

The performance of this system with the derived estimators and the GLRT detector was investigated by a set of experiments. The experiment site was chosen at one corner of the underground floor at IT University of Copenhagen. Figure 6 shows the site map. Three laptops equipped with ZyAIR B-100 802.11b cards were used as network nodes. The node positions and the directions of the WLAN cards are shown by the numbered triangles. One frame was transmitted per 2.5 ms. All the room walls were concrete and 25 cm thick. Three plastic laminated wooden doors A, B and C were chosen for experiments. Specifically, they were either closed or opened ( $30^\circ$ ) in order to produce small changes in the environment. The decision hypotheses were:  $\mathcal{H}_0$ : the chosen door was closed, and  $\mathcal{H}_1$ : the chosen door was opened. We compared the performance of this new system, which uses the adaptive estimator with Kalman filter and the GLRT detector, with the prototype system presented in [2]. To calculate the average probability of false alarm ( $P_f$ ),  $1.8 \times 10^5$  scanning cycles were recorded with all the doors closed. To calculate the average probability of detection ( $P_d$ ) of the door opening event, in experiment A, B and C, we opened the door A, B and C specifically and recorded 5000 scanning cycles in each case. Figure 7 shows the curve of the experimental results. As we can see,

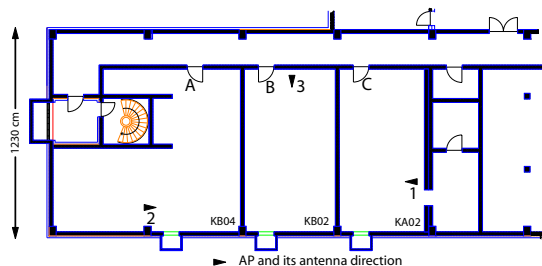


Figure 6: The experimental environment

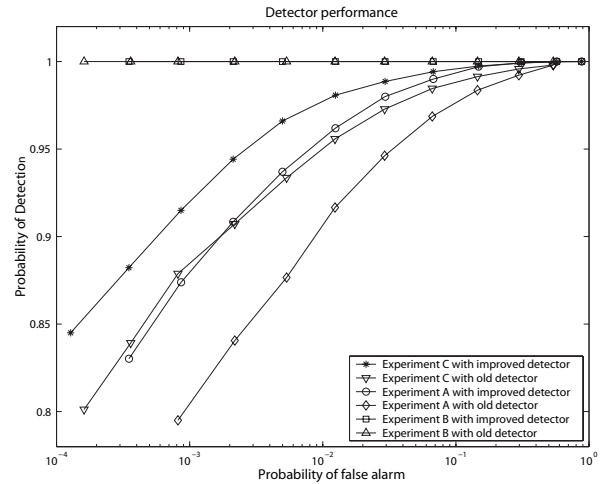


Figure 7: Performance comparison by experiments

for experiment B, both detectors performed very well and their difference is not visible. The reason was that door B was very close to node 3 and small changes at door B can produce significant signal strength changes at node 3, which were around 0.5 dB in the experiment B. In the more challenging experiment cases A and C, the largest signal strength changes, namely the largest  $\Delta l_{m,n}$  of all paths, were only around 0.2 dB. Therefore, the detection performance in experiment A and C was not good when the estimator and detector in [2] were applied. However, the system performance was improved significantly when the adaptive estimator and the change detector derived in this paper were applied. In experiments A and C, the  $P_f$  were reduced by nearly one order of magnitude at almost any probability of false alarm, for example when  $P_d = 0.9$  and  $P_d = 0.95$ .

## 8. CONCLUSIONS

We addressed the problem of using a multiple-node indoor wireless network as a distributed sensor network for detecting physical intruders into the indoor environment. We analyzed the challenges for achieving high performance of intrusion detection. We derived a high-precision adaptive parameter estimator with Kalman filter in Section 4, and we derived a high-precision signal level change estimator in Section 5. Experiments show that the detection performance of the derived system is significantly better than the published prototype multimodal wireless network system.

Given the low computational complexity of the estimators, we proposed a low-cost and robust system architecture, which eliminated the main constraints on deploying such kind of multimodal wireless network. The intrusion detection performance demonstrate that this novel application is promising, and the low-cost and robust system architecture make it possible for wide deployment.

## REFERENCES

- [1] K. Pahlavan, *Wireless Information Networks*, Wiley & Sons, 1995.
- [2] Z. Safar, J. Sørensen, J. Chen and K. Kristoffersen, "Multimodal Wireless Networks: Distributed Surveillance with Multiple Nodes", *IEEE International Conference on Acoustics, Speech and Signal Processing (ICASSP)*, Mar. 2005.
- [3] S. M. Kay, *Fundamentals of Statistical Signal Processing: Detection Theory*, Prentice-Hall, 1993.
- [4] I. Kollar, "Bias of Mean Value and Mean Square Value Measurements Based on Quantized Data", *IEEE Trans. Instrumentation and Measurement*, vol. 43, pp.733-739, Oct. 1994.
- [5] S. M. Kay, *Fundamentals of Statistical Signal Processing: Estimation Theory*, Prentice-Hall, 1993.
- [6] D. R. Cox and D. V. Hinkley, *Theoretical Statistics*, Chapman and Hall, 1974.